Jesus Ruiz, Andoni Lazkano, Jose Julio Gutiérrez, Luis Alberto Leturiondo, Izaskun Azcarate, Purificación Saiz, Koldo Redondo, "Influence of carrier phase on flicker measurement for rectangular voltage fluctuations", IEEE Transactions on Instrumentation and Measurement, Volume 61(3), 2012, Pages 629-635, ISSN 0018-9456, https://doi.org/10.1109/TIM.2011.2171611

(https://ieeexplore.ieee.org/abstract/document/6065755)

Abstract: This paper presents an analysis of the influence of the phase relationship between the fundamental frequency and the rectangular voltage fluctuation on flicker measurements made by the International Electrotechnical Commission (IEC) flickermeter. We analytically studied the origin of the deviations for a set of significant fluctuation frequencies. We found that the nonlinear behavior of the squaring multiplier of the IEC flickermeter produces an additional dc component in instantaneous flicker sensation *P*inst for several rectangular fluctuation frequencies. The value of this dc component depends on the phase relationship between the fundamental and the fluctuation frequency. The analysis of this paper has contributed to clarify the definition of some performance tests of the IEC flickermeter standard IEC 61000-4-15 ed.2. This will help develop calibration and verification methods for the flickermeters.

Keywords: Flicker, International Electrotechnical Commission (IEC) flickermeter, P_{st}, power quality, rectangular voltage fluctuation.

Influence of Carrier Phase on Flicker Measurement for Rectangular Voltage Fluctuations

J. Ruiz, *Member, IEEE,* A. Lazkano, *Member, IEEE,* J.J. Gutierrez, *Member, IEEE,* L.A. Leturiondo, *Member, IEEE,* I. Azkarate, *Student, IEEE,* P. Saiz and K. Redondo

***Abstract*—This paper presents an analysis of the influence of the phase relationship between the mains frequency and the rectangular voltage fluctuation on flicker measurements made by the IEC flickermeter. We studied analytically the origin of the deviations for a set of significant fluctuation frequencies. We found that the nonlinear behavior of Block 4 of the IEC flickermeter produces an additional DC component in the instantaneous flicker sensation, P_{inst}, for several rectangular fluctuation frequencies. The value of this DC component depends on the phase relationship between the mains frequency and the fluctuation frequency. The analysis of this work has contributed to clarify the definition of some Performance Tests of the IEC flickermeter standard IEC61000-4-15 ed.2. This will help to develop calibration and verification methods for the flickermeters.**

***Index Terms*—Power quality, flicker, IEC flickermeter, $\mathbf{P_{st}}$, rectangular voltage fluctuation.**

I. Introduction

VOLTAGE fluctuations in the power supply system cause variations of luminosity in light sources connected to the network. This phenomenon is known as *flicker* and is defined as the subjective perception of the irritation produced by these low-frequency fluctuations, for amplitudes within 10% of the nominal voltage. A flickermeter must quantify the annoyance induced in people by using a reference lamp to generate light fluctuations under supply voltage changes. Standard IEC 61000-4-15 [1] establishes the functional and design specifications for flickermeters, and defines the fundamental parameter for the measurement of the irritation, namely short-term flicker severity P_{st}.

Standard IEC 61000-3-3 [2] describes four types of voltage fluctuations introduced by the supply network: (a) periodic variations of voltage, with rectangular form and the same amplitude; (b) a series of variations of voltage irregularly distributed over time and amplitude; (c) clearly separated variations of voltage, which are not all stepped; and (d) random and continuous variations of voltage. This description typically corresponds to flicker sources in industrial electrical systems, such as arc furnaces inducing large irregular variations in current. However, smaller currents with regular working cycles must also be considered, such as those generated by heat pumps, welding machines, or the combined effect of several motors connected to the same line [3].

This work was supported by the Ministry of Science and Innovation (MICINN) of Spain through the project ENE2009-13978-C02-02, and by the Basque Goverment through the project IT425-10.

The authors are with the Electronics and Telecommunications Department of the University of the Basque Country (UPV/EHU), 48013 Bilbao, Spain. E-mail: andoni.lazkano@ehu.es

Since the first studies on flicker measurement [4]–[6], rectangular voltage fluctuations have been considered as the reference modulating functions for producing flicker. They have been studied in detail, and represent adequately both occasional abrupt changes and repetitive variations in voltage. They have also been used to define the threshold curve of annoyance [7], [8] and to fit the multipoint algorithm used to calculate the P_{st} parameter. The IEC flickermeter works specifically with this type of fluctuation in its operation tests. In the 2010 edition of this standard the operation tests are extended and many of them also use rectangular voltage fluctuations.

It is clear from reading the standard (and recently highlighted in [9]), that there are just two characteristics of voltage fluctuations that determine the annoyance level, and therefore the value of P_{st}, namely the frequency and the amplitude of the fluctuation. In this sense, the standard specifies that a flickermeter fulfilling the IEC design requirements must provide a unitary P_{st} measurement for several rectangular voltage fluctuations characterized by their amplitudes and frequencies.

The national metrology institutes have requested to go one step beyond, and a calibration and verification protocol has been projected by an IEC working group as a technical specification. This calibration system would allow to evaluate the performance of flickermeters not only for rectangular voltage fluctuations but also under more realistic conditions [10].

Neither the standard nor any recent studies on IEC flickermeter have considered whether the phase relationship between the carrier and the rectangular voltage fluctuation has an influence on the value of P_{st} [11]–[13]. This work analyzes the influence of the carrier phase on the P_{st} value generated by rectangular voltage fluctuations. Both experimental and analytical approaches are considered, and they reach the same conclusions.

In the remainder of this paper, Section II briefly introduces the IEC standard [1] and describes the implementation of the reference flickermeter used in this study. Section III presents our experimental results for analytically generated signals. Rectangular voltage fluctuation processing via the IEC flickermeter is analyzed theoretically in Section IV. This section also details a worst-case scenario. Section V contains a critical discussion of our results, with conclusions being stated in Section VI.

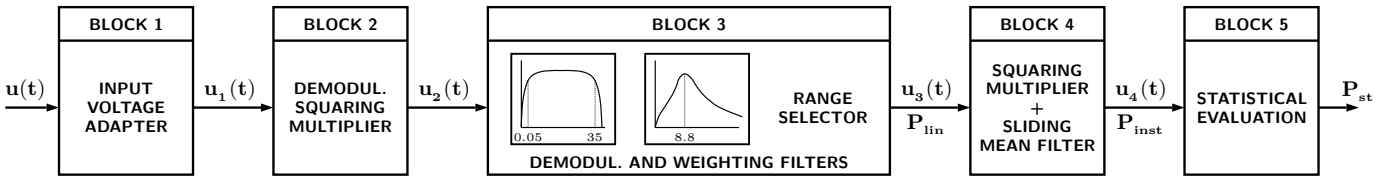

Fig. 1. Block diagram of the IEC flickermeter according to IEC 61000-4-15 [1].

II. Reference IEC flickermeter

Fig. 1 shows a block diagram of the IEC flickermeter according to the standard IEC 61000-4-15 [1]. In Block 1, the input voltage $u(t)$ is scaled to an internal reference value to make flicker measurements independent of input voltage level.

In Block 2, the scaled input voltage $u_1(t)$ is demodulated by means of a squaring multiplier. Block 3 comprises three cascaded filters. The first two filters complete the demodulation process and comprise a 1^{st} - order high-pass filter (3 dB cutoff frequency f_{co} = 0.05 Hz) and a 6^{th} - order low-pass Butterworth filter (3 dB cutoff frequency $f_{co,50}$ = 35 Hz for 50 Hz systems and $f_{co,60}$ = 42 Hz for 60 Hz systems). The third step is a band-pass filter that models the behavior of the lamp–eye system. The analogue response of this filter is given for both 230 V and 120 V reference lamps. The output of Block 3 is $u_3(t)$, which represents the weighted demodulated voltage-change signal P_{lin}.

Block 4 implements an eye–brain model. It includes a squaring multiplier followed by a low-pass filter that is specified to be a sliding-mean filter, having the transfer function of a 1^{st}-order low-pass resistance–capacitance filter with a time constant of 300 ms. The output of Block 4, $u_4(t)$, represents the instantaneous flicker sensation P_{inst}. A unit output from Block 4 corresponds to the reference human flicker perceptibility threshold. In Block 5, P_{st} is calculated by performing a statistical classification of P_{inst} over a short period of time (usually 10 min). The method for obtaining the P_{st} value is a multipoint algorithm that uses the percentiles obtained from the cumulative probability distribution of P_{inst}, namely

$$P_{st}=\sqrt{0.0314\cdot P_{0.1}+0.0525\cdot P_{1s}+0.0657\cdot P_{3s}+0.28\cdot P_{10s}+0.08\cdot P_{50s}}. \quad (1)$$

For the measurements performed in this work, we have implemented a highly accurate IEC flickermeter. This reference flickermeter is the complete digital MatLab implementation previously used in other studies [14]. Its three main features are: (a) it uses input sampling rates f_s = 1600, 3200, 6400 and 12800 $\frac{S}{s}$; (b) it performs a decimation process at the output of the low-pass demodulation filter to allow a constant sampling rate of 800 $\frac{S}{s}$ in the following blocks, independent of the input sampling rate; and (c) to avoid errors caused by the classification process, in terms of the number of classes, type of classification, or type of interpolation, the reference flickermeter does not classify the P_{inst} signal. Instead, it stores the 800 S/s of P_{inst} during the 10 min short-term period and calculates the percentiles for the P_{st} formula (1) in an absolutely accurate way.

III. Experimental results

In our experiments, we used a rectangular voltage fluctuation modulating a 50 Hz mains frequency, with a variable relationship between their phases. The input voltage signal $u(t)$ was generated analytically according to the expression

$$u(t) = V(1 + g_m^{BL}(t))\cos(\omega_o t + \varphi), \quad (2)$$

where V is the amplitude of the 50 Hz carrier $\omega_o = 2\pi 50$, φ is the initial phase of the carrier, and $g_m^{BL}(t)$ corresponds to the band-limited rectangular voltage fluctuation $g_m(t)$. Fig. 2 shows $g_m(t)$, with period $T_m = \frac{1}{fm}$ and amplitude $\frac{\Delta V}{V}$. In our experimental work, $g_m(t)$ was band-limited to avoid errors caused by aliasing effects. Using the cosine-Fourier representation, $g_m(t)$ and $g_m^{BL}(t)$ can be expressed analytically as

$$\left.\begin{aligned} g_m(t) &= \sum_{n=0}^{\infty} c_n \cos(n\omega_m t) \\ g_m^{BL}(t) &= \sum_{n=0}^{N} c_n \cos(n\omega_m t) \end{aligned}\right\} \; c_n = \tfrac{\Delta V}{V}\tfrac{2}{n\pi}\sin\left(\tfrac{n\pi}{2}\right), \quad (3)$$

where N is the greatest integer satisfying $Nf_m + f_o \le \frac{1}{2}f_s$.

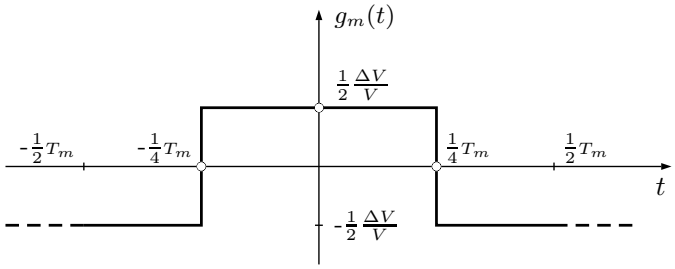

Fig. 2. Modulating rectangular voltage fluctuation of relative amplitude $\frac{\Delta V}{V}$ and frequency $f_m = \frac{1}{T_m}$.

The two extreme cases for the value of φ were studied experimentally. For $\varphi = 0$ rad, the carrier is a pure 50 Hz cosine function and, for $\varphi = \frac{3\pi}{2}$ rad, the carrier is a pure 50 Hz sine function. The effect on $u(t)$ is shown graphically in Fig. 3, for f_m = 25 Hz $\equiv$ 3000 changes per minute (cpm) and a carrier of 50 Hz. As shown in the expanded parts of the subfigures, there are clear differences in the way the discontinuity from the rectangular voltage fluctuation affects the signal $u(t)$.

Using the reference flickermeter, we calculated the P_{st} values produced by the signal $u(t)$ as f_m varied from 1 to 4000 cpm in steps of 1 cpm. The values of $\frac{\Delta V}{V}$ correspond to the unitary flicker severity measurements for the cosine carrier.

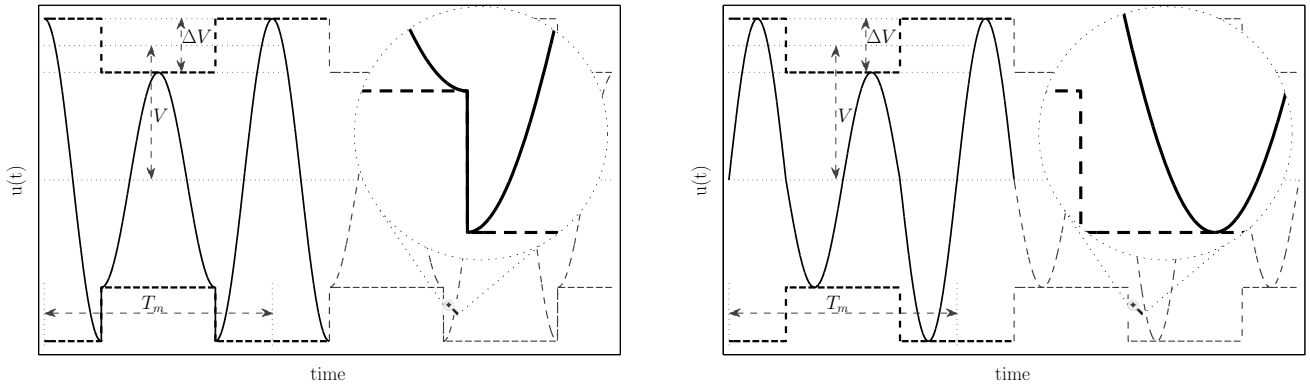

(a) $\varphi = 0$ rad. (b) $\varphi = \frac{3\pi}{2}$ rad.

Fig. 3. Waveform of $u(t)$ for a rectangular voltage fluctuation of 3000 cpm, $\frac{\Delta V}{V}$ = 40% and 50 Hz mains frequency. The phase relationship between the mains frequency and the rectangular voltage fluctuation is determined by φ.

The 4000 values of P_{st} for $\varphi = 0$ rad (cosine carrier), namely P_{stc}, and those corresponding to $\varphi = \frac{3\pi}{2}$ rad (sine carrier), namely P_{sts}, were obtained.

Fig. 4 shows the percentage deviation between P_{stc} and P_{sts} values, obtained as

$$\frac{\Delta P_{st}}{P_{st}} = 100 \cdot \frac{P_{sts} - P_{stc}}{P_{stc}}. \quad (4)$$

Ignoring the small deviations appearing for f_m between 2000 and 4000 cpm, it can be observed that, for most frequencies, the carrier phase does not influence the P_{st} value, given that the deviation between P_{stc} and P_{sts} is null. However, for some frequencies, the deviation is significant, surpassing 14% for f_m = 3000 cpm.

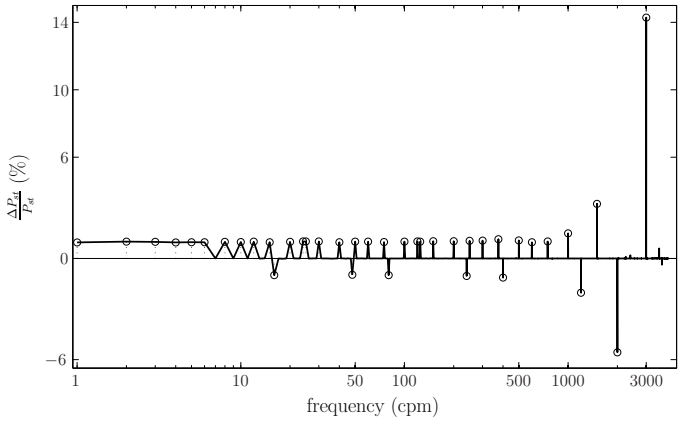

Fig. 4. Percentage deviation between P_{stc} and P_{sts} values using $\frac{\Delta V}{V}$ values corresponding to unitary flicker severity values for the cosine carrier, namely P_{stc} = 1.

Table I lists the range of frequencies with appreciable deviations. If the calculations are repeated for the maximum value of the instantaneous flicker sensation, namely $P_{inst,max}$, similar conclusions are obtained. Table I also shows the values of deviations obtained for $P_{inst,max}$ according to

$$\frac{\Delta P_{inst,max}}{P_{inst,max}} = 100 \cdot \frac{P_{insts,max} - P_{instc,max}}{P_{instc,max}}, \quad (5)$$

where $P_{insts,max}$ and $P_{instc,max}$ are the maximum values of P_{inst} for the sine and cosine carrier functions, respectively.

TABLE I
P_{st} AND $P_{inst,max}$ PERCENTAGE DEVIATIONS BETWEEN SINE AND COSINE CARRIERS.

f_m [1]	$\frac{\Delta P_{st}}{P_{st}}$ [2]	$\frac{\Delta P_{inst,max}}{P_{inst,max}}$ [3]	f_m	$\frac{\Delta P_{st}}{P_{st}}$	$\frac{\Delta P_{inst,max}}{P_{inst,max}}$
1	+0.96	+2.00	80	-0.99	-2.00
2	+0.95	+2.00	100	+1.00	+2.03
3	+0.99	+2.00	120	+1.01	+2.03
4	+0.95	+2.00	125	+1.00	+2.04
5	+0.96	+2.00	150	+1.02	+2.05
6	+0.96	+2.00	200	+1.02	+2.08
8	+0.98	+2.00	240	-1.03	-2.07
10	+0.98	+2.00	250	+1.04	+2.11
12	+1.00	+2.00	300	+1.05	+2.15
15	+0.96	+2.00	375	+1.14	+2.30
16	-1.00	-1.96	400	-1.14	-2.27
20	+0.99	+2.00	500	+1.07	+2.15
24	+1.00	+2.00	600	+0.96	+1.94
25	+1.00	+2.00	750	+1.01	+2.03
30	+1.00	+2.00	1000	+1.49	+2.98
40	+0.96	+2.00	1200	-2.03	-4.01
48	-0.97	-1.96	**1500**	**+3.24**	**+6.58**
50	+1.00	+2.00	**2000**	**-5.56**	**-10.81**
60	+0.99	+2.02	**3000**	**+14.28**	**+30.60**
75	+0.97	+2.02			

[1] f_m : fluctuation frequency in cpm
[2] $\frac{\Delta P_{st}}{P_{st}} = 100 \cdot \frac{P_{sts} - P_{stc}}{P_{stc}}$ in %
[3] $\frac{\Delta P_{inst,max}}{P_{inst,max}} = 100 \cdot \frac{P_{insts,max} - P_{instc,max}}{P_{instc,max}}$ in %

IV. THEORETICAL ANALYSIS

This section describes the theoretical framework used to explain and confirm the experimental results of the previous section. The intention is to obtain analytical expressions that can interpret the influence of the carrier phase on the value of $P_{inst,max}$ and P_{st} for different frequencies of the rectangular fluctuation.

The first block of the flickermeter scales $u(t)$ to its *rms* value, $V_{rms} = \frac{V}{\sqrt{2}}$, namely

$$u_1(t) = \sqrt{2}(1 + g_m^{BL}(t)) \cos(\omega_o t + \varphi). \quad (6)$$

The signal $u_1(t)$ is squared in Block 2. Given that the squared rectangular voltage fluctuation $(g_m^{BL}(t))^2$ is approxi-

mately a constant value of $\frac{1}{4}(\frac{\Delta V}{V})^2$, the output of Block 2 can be written as

$$\begin{aligned} u_2(t) \approx & \left[1+\tfrac{1}{4}(\tfrac{\Delta V}{V})^2+2g_m^{BL}(t)\right]\left[1+\cos(2\omega_o t+2\varphi)\right] \\ = & \Bigg[\overbrace{\left(1+\tfrac{1}{4}(\tfrac{\Delta V}{V})^2\right)}^{T_1}\Bigg]+\Bigg[\overbrace{\left(1+\tfrac{1}{4}(\tfrac{\Delta V}{V})^2\right)\cos(2\omega_o t+2\varphi)}^{T_2}\Bigg] \\ & +\Bigg[\underbrace{2g_m^{BL}(t)(1+\cos(2\omega_o t+2\varphi))}_{T_3}\Bigg]. \end{aligned} \tag{7}$$

The filters of Block 3 can be considered as a cascaded filter with a discrete frequency response $H_{eq}(\Omega)$. This equivalent system eliminates the DC component T_1, and strongly attenuates the T_2 component at $2f_o$. The spectral components that produce flicker are caused by term T_3. Using Equations (3) and (7), and considering the components in the range $0-2f_o$, the output of Block 3 can be represented as

$$\begin{aligned} u_3(t) \approx & 2\sum_{n_1=0}^{N_L} a_{n_1}\cos(n_1\omega_m t+\theta_{n_1}) \\ & +\sum_{n_2=0}^{2N_L} b_{n_2}\cos((n_2\omega_m-2\omega_o)t+\theta_{n_2}-2\varphi), \end{aligned} \tag{8}$$

where N_L is the greatest integer satisfying $f_m \cdot N_L \leq 2f_o$ and

$$\begin{aligned} a_{n_1} &= c_{n_1}\cdot\left|H_{eq}(\Omega)\right|_{\Omega=n_1\omega_m} \\ \theta_{n_1} &= \angle\big(H_{eq}(\Omega)\big)\big|_{\Omega=n_1\omega_m} \\ b_{n_2} &= c_{n_2}\cdot\left|H_{eq}(\Omega)\right|_{\Omega=n_2\omega_m-2\omega_o} \\ \theta_{n_2} &= \angle\big(H_{eq}(\Omega)\big)\big|_{\Omega=n_2\omega_m-2\omega_o} \end{aligned}. \tag{9}$$

In Block 4, the signal $u_3(t)$ is squared and low-pass filtered with a 3 dB cutoff frequency of 0.53 Hz. For this reason, the DC component of $u_3(t)$ contributes decisively to the final waveform of the instantaneous flicker sensation and therefore to the values of $P_{inst,max}$ and P_{st}.

In general, when the sum of two spectral components, w_1 and w_2, is squared, the resulting signal contains a DC component that depends on the relation between w_1 and w_2, as given by

$$x(t) = A_1\cos(\omega_1 t)+A_2\cos(\omega_2 t), \tag{10}$$

$$DC_{x^2} = \begin{cases} \frac{A_1^2+A_2^2}{2} & |\omega_1| \neq |\omega_2| \\ \frac{A_1^2+A_2^2}{2}+A_1A_2 & |\omega_1| = |\omega_2|. \end{cases} \tag{11}$$

This consideration can be applied to the squaring of $u_3(t)$. The spectral components of the first term of Equation (8) will give rise to results related to the condition $|\omega_1| \neq |\omega_2|$ of Equation (11). However, the DC components caused by the cross-products between both terms of Equation (8) are related to the condition $|\omega_1| = |\omega_2|$ of Equation (11). This condition can be met for two values of n_2, namely

$$\begin{aligned} n_1\omega_m = n_2^{'}\omega_m - 2\omega_o \Rightarrow n_2^{'} &= \tfrac{2\omega_o+n_1\omega_m}{\omega_m} \\ n_1\omega_m = 2\omega_o - n_2^{''}\omega_m \Rightarrow n_2^{''} &= \tfrac{2\omega_o-n_1\omega_m}{\omega_m}. \end{aligned} \tag{12}$$

For the f_m values implied by Equation (12), $u_3(t)$ in Equation (8) will contain three terms of the form

$$\begin{aligned} s(t) = & 2a_{n_1}\cos(n_1\omega_m t+\theta_{n_1}) \\ & + b_{n_2}^{'}\cos\left((n_2^{'}\omega_m-2\omega_o)t+\theta_{n_2}^{'}-2\varphi\right) \\ & + b_{n_2}^{''}\cos\left((2\omega_o-n_2^{''}\omega_m)t+\theta_{n_2}^{''}-2\varphi\right). \end{aligned} \tag{13}$$

We can make the simplifications

$$\begin{aligned} \omega_1 &= n_1\omega_m = n_2^{'}\omega_m-2\omega_o = 2\omega_o-n_2^{''}\omega_m \\ A_1 &= 2a_{n_1} \\ A_2 &= b_{n_2}^{'} \\ A_3 &= b_{n_2}^{''} \\ \theta_1 &= \theta_{n_1} = \theta_{n_2}^{'} = -\theta_{n_2}^{''} \end{aligned} \tag{14}$$

resulting in

$$\begin{aligned} s(t) = & A_1\cos(\omega_1 t+\theta_1)+A_2\cos(\omega_1 t+\theta_1-2\varphi) \\ & + A_3\cos(-\omega_1 t-\theta_1-2\varphi). \end{aligned} \tag{15}$$

The DC component provided by $s^2(t)$ can then be expressed as

$$\begin{aligned} DC_{s^2} = & \tfrac{A_1^2+A_2^2+A_3^2}{2}+(A_1A_2+A_1A_3)\cos(2\varphi) \\ & + A_2A_3\cos(4\varphi). \end{aligned} \tag{16}$$

For the extreme cases corresponding to the cosine carrier ($\varphi = 0$ rad) and the sine carrier ($\varphi = \frac{3\pi}{2}$ rad), the DC component of the output of Block 4 is made up of terms of the form

$$\begin{aligned} DC_{s^2} = & \tfrac{A_1^2+A_2^2+A_3^2}{2}+A_2A_3+A_1(A_2+A_3) \quad \text{if } \varphi = 0 \\ DC_{s^2} = & \tfrac{A_1^2+A_2^2+A_3^2}{2}+A_2A_3-A_1(A_2+A_3) \quad \text{if } \varphi = \tfrac{3\pi}{2}. \end{aligned} \tag{17}$$

The values of f_m fulfilling Equation (12) can be obtained as

$$n_1\omega_m = |n_2\omega_m-2\omega_o| \Rightarrow f_m = \frac{2f_o}{|n_1 \pm n_2|}. \tag{18}$$

Because the indexes n_1 and n_2 are odd, the combination $|n_1 \pm n_2|$ is always an even number. The singular frequencies that produce $P_{inst,max}$ and P_{st} values depending on the carrier phase are given by

$$f_m = \frac{2f_o}{2n+2} \equiv \frac{12000}{2n+2} \text{ cpm} \quad \text{for} \quad f_m \in \mathbb{N},\ n = 1,2,3,.... \tag{19}$$

The results provided by Equation (19) are exactly the frequencies that were detected experimentally and listed previously in Table I. It is therefore verified analytically that the deviation in $P_{inst,max}$ and P_{st} that depends on the carrier phase is caused by an additional DC component that appears in P_{inst} for those values of f_m that generate identical components in both terms of Equation (8).

A. Case study for fm=3000 cpm

In this subsection, the case of f_m = 25 Hz $\equiv$ 3000 cpm, which produced the largest deviation between the sine and the cosine carriers (see Table I), is analyzed in detail.

If we ignore the components above $3f_m$ = 75 Hz at the output of Block 3, which will be strongly attenuated by the Block 3 filters, Equation (8) can be expressed as

$$u_3(t) \approx 2a_1\cos(\omega_m t+\theta_1)+b_3\cos(-\omega_m t+\theta_3-2\varphi) + b_5\cos(\omega_m t+\theta_5-2\varphi). \quad (20)$$

Because $\theta_3=-\theta_1$ and $\theta_5=\theta_1$, this can be rewritten as

$$u_3(t) \approx 2a_1\cos(\omega_m t+\theta_1)+b_3\cos(\omega_m t+\theta_1+2\varphi) + b_5\cos(\omega_m t+\theta_1-2\varphi). \quad (21)$$

On squaring $u_3(t)$ in Block 4, a DC component and a component at $2f_m$ (50 Hz), which is strongly attenuated by the low-pass filter of Block 4, are obtained. Therefore, the output of Block 4 can be approximately given by a DC component, of the form

$$u_4(t) \approx 2a_1^2+\tfrac{b_3^2}{2}+\tfrac{b_5^2}{2}+2a_1(b_3+b_5)\cos(2\varphi)+b_3b_5\cos(4\varphi). \quad (22)$$

The way in which the carrier phase φ affects P_{inst} is therefore verified. P_{inst} is a DC component, but its value depends on φ. For a cosine carrier (φ = 0 rad), the output of Block 4 is given by

$$u_4(t) \approx 2a_1^2+\tfrac{b_3^2}{2}+\tfrac{b_5^2}{2}+2a_1(b_3+b_5)+b_3b_5, \quad (23)$$

whereas for the sine carrier ($\varphi=\frac{3\pi}{2}$ rad), it is

$$u_4(t) \approx 2a_1^2+\tfrac{b_3^2}{2}+\tfrac{b_5^2}{2}-2a_1(b_3+b_5)+b_3b_5. \quad (24)$$

Using the reference flickermeter, if $P_{inst,max}$ is evaluated experimentally as a function of φ for a rectangular voltage fluctuation of f_m = 3000 cpm, a constant value should be obtained, caused by the first term in Equation (22), upon which the sum of a cosine of 2φ and another of 4φ are superimposed.

The upper plot of Figure 5 shows, as solid line, the experimental $P_{inst,max}$ values obtained when the carrier phase varies from 0 to 2π rad. We applied a 3000 cpm rectangular voltage fluctuation with an amplitude that produces a unitary $P_{inst,max}$ value for a cosine carrier (that is, $P_{instc,max}$ = 1). The upper plot of Figure 5 shows, as dashed line, the theoretical values provided by Equation (22). A small difference between the experimental and theoretical values can be observed. This difference comes from the 50 Hz component produced by the squaring of $u_3(t)$ in Block 4. Although the low-pass filter of Block 4 strongly attenuates this component, it remains in P_{inst}. The deviation obtained for the theoretical values of $P_{inst,max}$ in the two extreme cases of φ = 0 and $\varphi=\frac{3\pi}{2}$ is 30.61%, which is consistent with the values listed in Table I.

The lower plot of Figure 5 shows the P_{inst} waveform during a 0.1 s period, provided by the reference flickermeter for $\varphi=0$, $\frac{\pi}{4}$ and $\frac{3\pi}{2}$ rad. The P_{inst} waveform is almost identical for the three cases, namely a small 50 Hz component superimposed on a DC component. The 50 Hz component has some influence on the $P_{inst,max}$ value, although it was ignored in Equation (22).

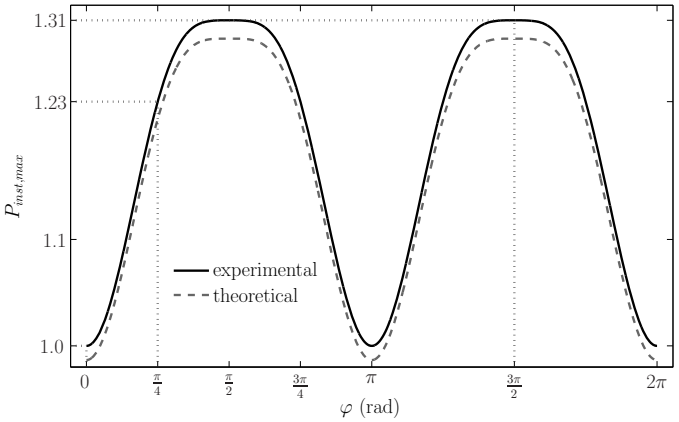

(a) Maximum values of P_{inst} depending on φ.

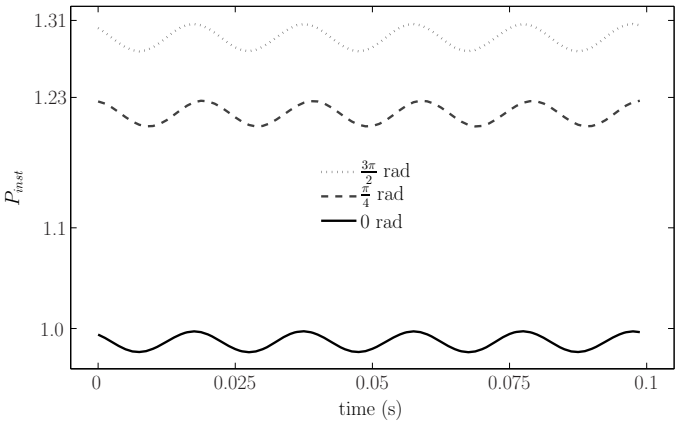

(b) P_{inst} waveform.

Fig. 5. $P_{inst,max}$ and P_{inst} for a rectangular voltage fluctuation of 3000 cpm $\frac{\Delta V}{V}$ = 0.8779%, depending on the carrier phase φ.

V. Discussion of the Results

The previous IEC standard [15] specifies operational tests for the instantaneous flicker sensation P_{inst} and for the short-term flicker severity P_{st}. For rectangular voltage fluctuations, the standard considers the calculation of $P_{inst,max}$ for the various frequencies listed in Table I: 60, 120, 240, 300, 600, and 1200 cpm (0.5, 1, 2, 2.5, 5, and 10 Hz). The deviation in $P_{inst,max}$ that the carrier phase produces at these frequencies is less than 4%. This error is within the tolerance of 5% permitted by the standard. For P_{st}, the standard requires analysis of the behavior of the flickermeter for seven rectangular voltage fluctuations. Only the frequencies of 1 and 2 cpm coincide with those listed in Table I. The deviation generated by the carrier phase at these frequencies is less than 1%, which is below the tolerance of 5% permitted by the standard.

The TF1 group belonging to WG2 (Voltage fluctuations and other low-frequency phenomena) of the IEC SC77A subcommittee has been working on an update to the IEC 61000-4-15 standard. The new 2010 edition of the IEC standard [1] demands more exhaustive operational tests. In the tests specified for checking the normalized flickermeter response ($P_{inst,max}$ = 1) for rectangular voltage fluctuations, the frequency of 3000 cpm is included. In this case, the

deviation between cosine and sine carriers is over 30%. To solve this problem, the new standard explicitly indicates that a sine carrier must be used. The values of fluctuation amplitude provided by the standard are calculated using the sine carrier.

Since the first studies carried out on flicker [4]–[6], sinusoidal and rectangular voltage fluctuations have been used and studied in detail. In these cases, using a reference lamp, it has been experimentally verified that the degree of annoyance suffered by people depends exclusively on the amplitude and frequency of the fluctuations. Actual annoyance is therefore independent of the carrier phase. The deviations observed in $P_{inst,max}$ and P_{st} for rectangular voltage fluctuations in Table I depend on the carrier phase, demonstrating undesirable behavior in a flickermeter. The origin of the deviation is the squaring operation of Block 4. Even if the influence of the carrier phase on the measurement of P_{st} in real situations is difficult to determine, we believe that it should be taken into account when using the IEC flickermeter with rectangular voltage fluctuations.

The preliminary studies reported in this work concerning the influence of the carrier phase on rectangular voltage fluctuations have been communicated to WG2 of the IEC SC77A subcommittee, with the aim of analyzing this dependency in depth and minimizing undesired effects in the future.

VI. Conclusions

We have given a full analysis of the influence of the 50 Hz carrier phase on the values of $P_{inst,max}$ and P_{st} provided by the IEC flickermeter when working with rectangular voltage fluctuations. The study was carried out experimentally by using a high-precision IEC flickermeter with analytically generated signals. The experimental results have been confirmed and justified by analysis. The work has explained how values related to a set of fluctuation frequencies can be influenced by the phase relationship between the carrier and the modulating function. This influence can produce deviations of 14% for P_{st} and up to 30% for $P_{inst,max}$.

In reality, for a given type of lamp, the annoyance caused in people by rectangular supply voltage fluctuations depends exclusively on the frequency and amplitude of the fluctuation. For this reason, we believe that the results obtained demonstrate undesirable behavior by the IEC flickermeter, which should be taken into account. The results of this work, together with previous research [14] could be used to improve some aspects of the IEC flickermeter.

References

[1] IEC-61000-4-15ed2.0, "Electromagnetic compatibility (EMC) part 4: Testing and measurement techniques - section 15: Flickermeter functional and design specifications," 2010.

[2] IEC-61000-3-3, "Electromagnetic compatibility (EMC) part 3: Limits - section 3: Limitation of voltage changes, voltage fluctuations and flicker in public low-voltage supply systems, for equipment with rated current less than 16A per phase and not subject to conditional connection," 2008.

[3] P. Q. W. . UIE, "Guide to quality of electrical supply for industrial installations. Part 5: Flicker," 1997, Tech. Rep.

[4] M. Ailleret, "Détermination des lois expérimentales du papillotement (flicker) en vue de leur application aux réseaux basse tension sur lesquels les charges varient priodiquement ou aléatoirement (soudeuses démarrages de moteurs)," *Bulletin de la Société Franaise des Electriciens*, vol. 7, no. 77, 1957.

[5] H. de Lange, "Eye's response at flicker fusion to square-wave modulation of a test field surrounded by a large steady field of equal mean luminance," *Journal of the Optical Society of America*, vol. 51, no. 4, pp. 415–421, 1961.

[6] C. Rashbass, "The visibility of transient changes of luminance," *The Journal of Physiology*, vol. 210, no. 1, p. 165, 1970.

[7] IEC-555-3, "Disturbances in supply systems caused by household appliances and similar electric equipment - part 3: Voltage fluctuations." 1982.

[8] G. Cornfield, "Definition and measurement of voltage flicker," *Electronics in Power Systems Measurement, IEE Colloquium on*, p. 4, 1988.

[9] P. Clarkson and P. Wright, "The calibration of IEC standard flickermeters using complex modulated signals," *IEEE Trans. Instrum. Meas.*, vol. 58, no. 4, pp. 1017–1022, 2009.

[10] P. Espel, "Comparison of three accurate methods for flicker measurements," *Metrologia*, vol. 47, no. 3, pp. 287–294, Jun. 2010.

[11] G. Wiczynski, "Simple Model of Flickermeter Signal Chain for Deformed Modulating Signals," *IEEE Trans. Power Del.*, vol. 23, no. 4, pp. 1743–1748, 2008.

[12] D. Gallo, C. Landi, R. Langella, and A. Testa, "On the Use of the Flickermeter to Limit Low-Frequency Interharmonic Voltages," *IEEE Trans. Power Del.*, vol. 23, no. 4, pp. 1720–1727, 2008.

[13] G. Chang, C. Chen, and Y. Huang, "A Digital Implementation of Flickermeter in the Hybrid Time and Frequency Domains," *IEEE Trans. Power Del.*, vol. 24, no. 3, pp. 1475–1482, 2009.

[14] J. Ruiz, J. Gutierrez, A. Lazkano, and S. Ruiz de Gauna, "A review of flicker severity assessment by the iec flickermeter," *IEEE Trans. Instrum. Meas.*, vol. 59, no. 8, pp. 2037–2047, aug. 2010.

[15] IEC-61000-4-15ed1.1, "Electromagnetic compatibility (EMC) part 4: Testing and measurement techniques - section 15: Flickermeter functional and design specifications," 2003.